

<https://doi.org/10.31896/k.28.2>

Original scientific paper

Accepted 21. 8. 2024.

**GUNTER WEISS
BORIS ODEHNAL**

Miquel's Theorem and its Elementary Geometric Relatives

Miquel's Theorem and its Elementary Geometric Relatives

ABSTRACT

The elementary geometric Miquel theorem concerns a triangle $\triangle ABC$ and points R, S, T on its sides, and it states that the circles $k(ART)$, $k(BRS)$, $k(CST)$ have a common point M , the Miquel point to these givens. Choosing R, S, T in special ways one receives the so-called *beermat theorem*, the *Brocard theorems*, and the *Steiner Simson-Wallace theorem* as special cases of Miquel's theorem. Hereby facts connected with Brocard's theorem follow from properties of Miquel's theorem. If e.g. R, S, T fulfill the Ceva condition, Miquel's construction induces a mapping of the Ceva point to the Miquel point. We discuss this and other mappings, which are natural consequences of Miquel's theorem. Furthermore, if the points R, S, T run through the sides of \triangle such that e.g. the affine ratios $ar(ARB)$, $ar(BSC)$, $ar(CTA)$ are equal, then the corresponding Miquel points M run through the circumcircle of the triangle formed by the Brocard points and the circumcenter of \triangle . Besides these three remarkable points of \triangle , this circle contains several other triangle centers. Even though most of the presented topics are well-known, their mutual connections seem to be not yet considered in standard references on triangle geometry and therefore might justify an additional treatment.

Key words: Miquel's theorem, Brocard's theorems, theorems of Steiner and Simson-Wallace

MSC2010: 51M04, 51N15

Miquelov teorem i njegovi elementarnogeometrijski srodnici

SAŽETAK

Elementarnogeometrijski Miquelov teorem odnosi se na trokut $\triangle ABC$ i točke R, S, T na njegovim stranicama, i kaže da kružnice $k(ART)$, $k(BRS)$, $k(CST)$ imaju jednu zajedničku točku M , Miquelovu točku zadane figure. Posebnim odabirom točaka R, S, T dobivaju se takozvani *beermat teorem*, *Brocardovi teoremi* i *Steinerov Simson-Wallaceov teorem* kao specijalni slučajevi Miquelovog teorema. Stoga, činjenice vezane za Brocardov teorem slijede iz svojstava Miquelovog teorema. Ako npr. R, S, T zadovoljavaju Cevin uvjet, Miquelova konstrukcija inducira preslikavanje Cevine točke u Miquelovu točku. Proučavamo ovo i druga preslikavanja koja su direktna posljedica Miquelovog teorema. Nadalje, kreću li se točke R, S, T stranicama trokuta tako da su npr. afini omjeri $ar(ARB)$, $ar(BSC)$, $ar(CTA)$ jednaki, Miquelove točke M opisuju kružnicu opisanu trokutu čiji su vrhovi dvije Brocardove točke i središte opisane kružnice trokuta. Osim spomenutih triju posebnih točaka trokuta, na ovoj kružnici leži još nekoliko osobitih točaka trokuta. Iako je većina predstavljenih tema dobro poznata, čini se da njihove međusobne veze još nisu razmatrane u standardnoj literaturi iz geometrije trokuta i stoga bi mogle opravdati dodatnu obradu.

Ključne riječi: Miquelov teorem, Brocardovi teoremi, Steinerovi Simson-Wallaceovi teoremi

1 Introduction

In 1838 Auguste Miquel (1816-1851) published a theorem (see [10]), which later on was called after him and got the meaning of an important axiom in circle geometries, see e.g. [2]. (In [11] it is mentioned, that this remarkable incidence was known already since 1804.) The elementary geometric version of Miquel's theorem concerns a triangle $\triangle ABC$ and an inscribed triangle $\triangle RST$, and it states that

the circles $k(ART)$, $k(BRS)$, $k(CST)$ have a common point M , the *Miquel point* to these givens, see Fig. 1. For M there exists a two-parametric set of possibilities, such that there is a one-parameter family of triplets R, S, T to a given point M . The consequences of this fact are properties of the Miquel configuration and *Miquel mappings*, which seemingly are not yet considered. This will be treated in Chapter 2. Obviously, when choosing R, S, T dependent (e.g. collinear or infinitesimally close to the vertices A, B, C), the cor-

responding Miquel point M will get special meanings and connect Miquel's theorem to e.g. that of Steiner and Simson-Wallace resp. to Brocard's theorems. The well-known *beer-mat theorem* and it's reverse, the *three circle theorem*, is a relative of Miquel's theorem, too. We dedicate Chapter 3 to these rather well-known 2-dimensional cases.

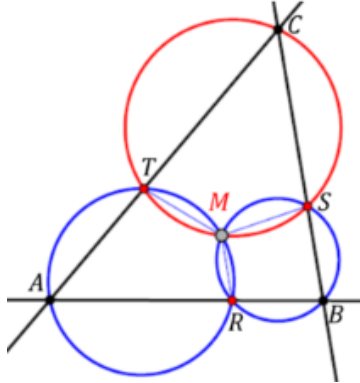


Figure 1: Elementary geometric version of Miquel's theorem

If the points R, S, T run through the sides of \triangle such that e.g. the affine ratios $ar(ARB)$, $ar(BSC)$, $ar(CTA)$ are equal, then the corresponding Miquel points M run through the circumcircle of the triangle formed by the Brocard points and the circumcenter of \triangle . Besides these three remarkable points of \triangle , this circle contains several other triangle centers. This will be the content of Chapter 4. Here, we refrain from presenting further generalizations, as, for example, using congruent point series on the sides of \triangle or cross ratios instead of the affine ratios. This will be treated at another occasion.

Finally, it is well-known that the theorem of Miquel holds in classical circle geometries, but it also holds in affine normed planes, while it is not true in an elliptic or hyperbolic plane. We show some examples in Chapter 5.

2 Properties of elementary geometric Miquel figures

2.1 Miquel stars to a given triangle

To an arbitrarily chosen point M , we construct the feet R, S, T on the sides of $\triangle ABC$. The Miquel circles $k(ART)$, $k(BRS)$, $k(CST)$ then are the Thales circles over segments $[MA]$, $[MB]$, $[MC]$, and M is indeed their common intersection. Therewith, as the lines RM, SM, TM are parallel to the altitudes of $\triangle ABC$, they include angles $\angle RMT = \pi - \alpha$, $\angle RMS = \pi - \beta$, $\angle SMT = \pi - \gamma$, see Fig. 2. Choosing another point $R' \in AB$ leads to Miquel circles $k(AR'M)$, $k(BR'M)$, which intersect BC in S' and CA in T' , see Fig. 2.

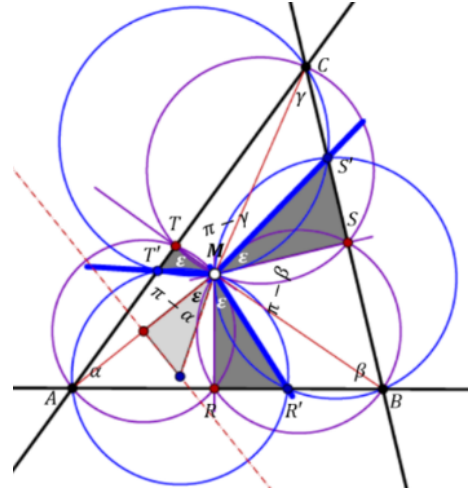


Figure 2: The triples (R, S, T) , (R', S', T') , belonging to a fixed Miquel point M define congruent Miquel stars.

For quadrangles inscribed into these circles, opposite angles must sum up to π , and therefore $\angle RMR' = \angle SMS' = \angle TMT'$. In the following we use

Definition 1 Let M be the Miquel point of a triangle $\triangle ABC$ to R', S', T' . The triplet of half-lines (MR', MS', MT') is called the Miquel star associated with the point M .

For Miquel stars the following holds

Theorem 1 If R' runs through AB , the Miquel star rotates about M with angle ϵ . The Miquel stars to different Miquel points are congruent, i.e. the angles enclosed by any pair of half-lines are equal.

The content of Theorem 1 relates to generalizations of Wallace's theorem, see [11]. The vertex triplets R', S', T' , belonging to a given Miquel-point M , form triangles, the sides of which envelop three parabolas with common focus M . (This follows from the projectivity between e.g. $R' \in AB \mapsto S' \in BC$.) The trilateral of vertex-tangents of the parabolas has the pedal points R, S, T of M for its vertices, and the directrices pass through the reflection images R'', S'', T'' of M in the sides of $\triangle ABC$, see Fig. 3. Therewith follows

Theorem 2 Let M be given and let R' run through AB . Then the sides of $\triangle R'S'T'$ envelop three parabolas with common focus M . Their common chords form a complete quadrangle consisting of the incenter I and the excenters of $\triangle R''S''T''$. (R'', S'', T'' are the images of reflections of M in the sides of $\triangle ABC$, and $\triangle R''S''T''$ consists of the directrix lines of the above mentioned parabolas.)

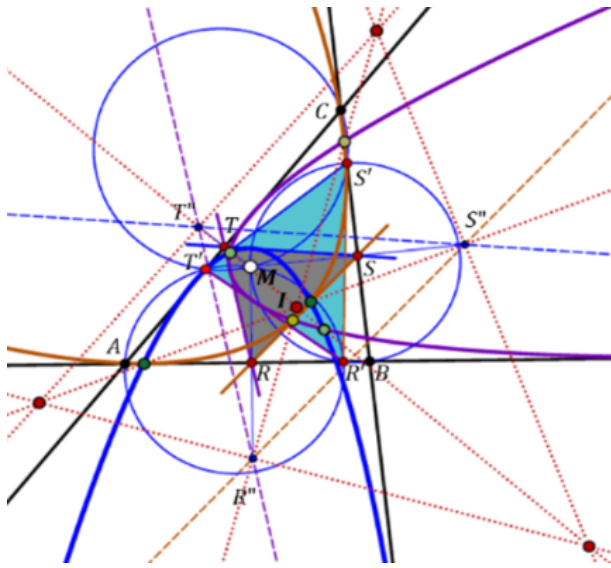


Figure 3: The sides of $\triangle R'S'T'$ envelop three parabolas with common focus M . Their common chords form a complete quadrangle.

2.2 A first Miquel mapping

The chords through the real intersection points of pairs of parabolas turn out to be the interior angle bisectors of triangle $R''S''T''$. Therefore, the common intersection point I of the three cords is the incenter of $R''S''T''$. As two parabolas intersect (in algebraic sense) in 4 points, there must exist, for our three parabolas, a complete quadrangle formed by six chords, see Fig. 3. It is near laying that the outer chords then must be the second angle bisectors of $R''S''T''$ and deliver the excenters. It makes sense to define a *first Miquel mapping*:

Definition 2 Given a triangle $\triangle ABC$ and an arbitrarily given point M . Reflecting M in the sides of $\triangle ABC$ delivers a triangle $R''S''T'' =: \triangle''$. The first Miquel mapping μ_1 to $\triangle ABC$ maps the point M to the incenter I of the reflection triangle \triangle'' of M .

Remark 1 When we choose R, T, S as (collinear) ideal points, then the three degenerate Miquel circles consist of a side of $\triangle ABC$ together with the ideal line. The ideal line is therefore a common one-dimensional component and a Miquel point M is not defined. But when we choose an ideal point as Miquel point, points R'', S'', T'' are constructible, as reflections, extended to ideal points, act as harmonic homologies. Incenter and excenters to this degenerate ideal triangle \triangle'' are not defined. The triangle \triangle'' collapses, too, if M is a point of the circumcircle c of $\triangle ABC$. Let $M \in c \setminus \{A, B, C\}$, then $R'' \neq S'' \neq T'' \neq R''$ are

collinear and define a segment bounded by two of the points R'', S'', T'' , while the third, inner point, can act as limit of the incenter I of \triangle'' . (The limits of the excenters E_i are the other two vertices plus the ideal point of the direction orthogonal to line $R''S''$. Therefore, the exceptional set for the first Miquel mapping μ_1 consist of $\{A, B, C\}$ alone.

Without calculation, by arguments of elementary geometry and chains of projectivities, we find that

- the orthocenter O and the vertices A, B, C are fixed points of the first Miquel mapping μ_1 ,
- a point M at the circumcircle c of \triangle is mapped to a point I on one of the circular arcs $(AOB), (BOC), (COA)$ of circles congruent to c , (obviously, the triangles \triangle'' then collapse to lines through O), see Fig. 4,
- if M traverses through a side of \triangle , e.g. through AC , then I runs along conic arcs through A and C , see Fig. 5a. Here I and one excenter E_i swap their meaning for inner resp. outer points M of the segment $[A, C]$. The pairs $(I, E_1), (E_2, E_3)$ run through two conics.

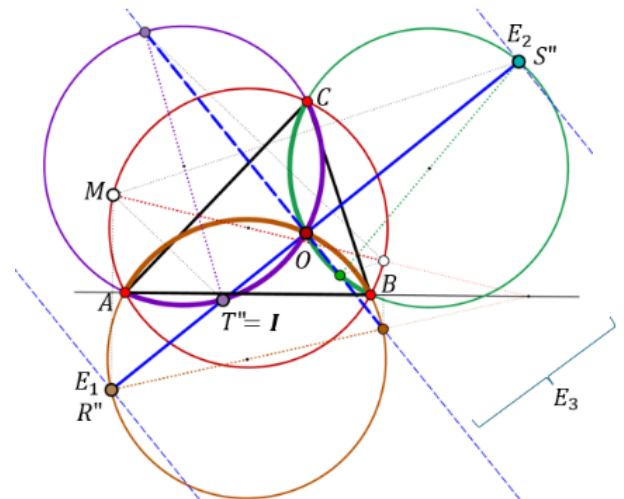


Figure 4: The first Miquel-mapping μ_1 maps a point M on the circumcircle c to a point I on one of the circular arcs AOB, BOC, COA of circles congruent to c . The “excenters” trace the remaining arcs of these circles plus the ideal line. The orthocenter O and A, B, C are mapped to themselves.

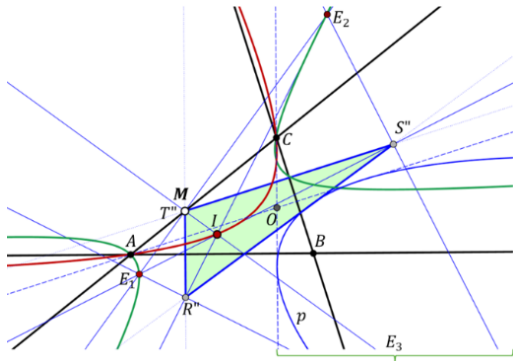


Figure 5a: If M runs through a side of $\triangle ABC$, e.g. through AC , then the incenters and excenters of \triangle'' run through a pair of conics through A and C . The line $R''S''$ envelops a parabola p with focus B and touching the altitudes of $\triangle ABC$ through A, C .

The following figures Fig. 5b and Fig. 5c show general cases of the mapping μ_1 . It seems that, when M traces a line l , the orbits of I and E_i are parts of one algebraic curve.

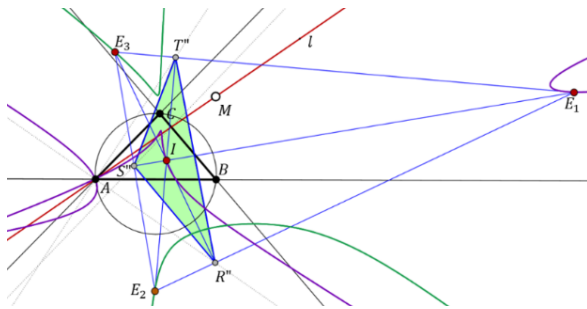


Figure 5b: If M runs through a line l through A , then I and E_i to \triangle'' run in pairs through two parts of an algebraic curve.

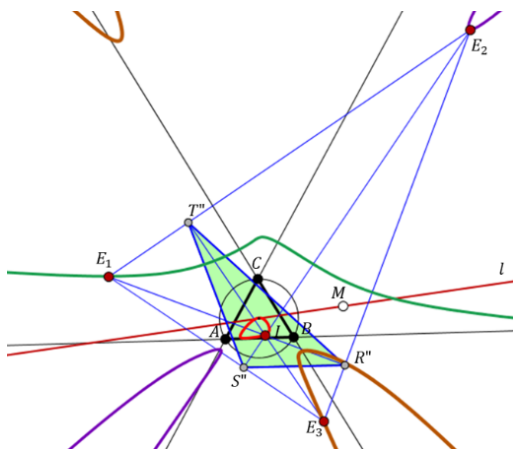


Figure 5c: If M runs through a line l not passing through a vertex of $\triangle ABC$, then I and E_i trace four distinct parts of an algebraic curve, such that the mapping $\mu_1 : M \mapsto I$ is independent of E_i . In the presented case, I traces even a closed curve.

For an analytic description of μ_1 it seems adequate to connect a Cartesian frame with the triangle $\triangle ABC$ with origine A and unit point B on the x -axis. Thus, $\triangle ABC$ as also $\triangle AMB$ can be described by the angles α and β (fixed) resp. ξ and η (variable), see Fig. 6. With these angles the side lengths a, b are

$$a = \frac{\sin \alpha}{\sin(\alpha + \beta)}, \quad b = \frac{\sin \beta}{\sin(\alpha + \beta)}, \quad c = 1 \tag{1}$$

$$|AM| = \frac{\sin \eta}{\sin(\xi + \eta)},$$

$$|BM| = \frac{\sin \xi}{\sin(\xi + \eta)},$$

$$|CM| = \frac{\sin(\alpha - \eta) \sin \beta}{\sin(\xi + \eta) \sin \sphericalangle AMC}, \tag{2}$$

$$(\cot \sphericalangle AMC = \frac{\sin \alpha \sin(\beta - \eta) + \cos(\xi + \eta) \sin \beta \sin(\alpha - \xi)}{\sin \beta \sin(\alpha - \xi) \sin(\xi + \eta)}),$$

$$|R''T''| = 2|AM| \sin \alpha,$$

$$|R''S''| = 2|BM| \sin \beta,$$

$$|S''T''| = 2|CM| \sin(\alpha + \beta), \tag{3}$$

$$R'' = |AM| \begin{pmatrix} \cos \xi \\ -\sin \xi \end{pmatrix},$$

$$T'' = |AM| \begin{pmatrix} \cos(2\alpha - \xi) \\ -\sin(2\alpha - \xi) \end{pmatrix},$$

$$S'' = |BM| \begin{pmatrix} 1 - \cos(2\beta - \eta) \\ \sin(2\beta - \eta) \end{pmatrix}. \tag{4}$$

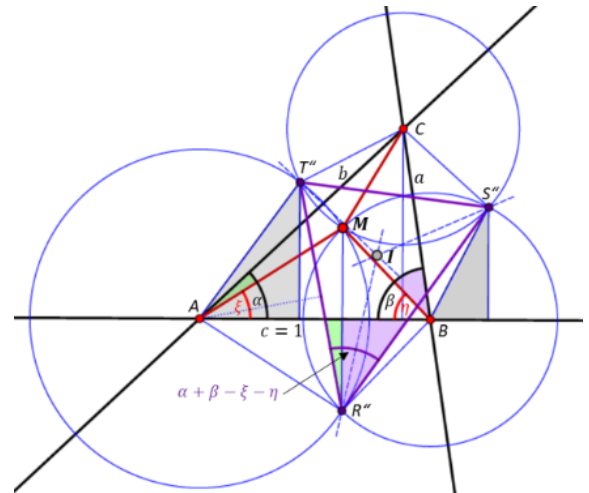


Figure 6: Labeling used for calculating the analytic representation of the first Miquel mapping μ_1 .

When iterating $\mu_1 : M \mapsto I =: M^1 \mapsto I^1 =: M^2 \rightarrow \dots$, we might suppose the following

Conjecture: The orthocenter O of $\triangle ABC$ is an attractor of μ_1^n , ($n \rightarrow \infty$).

Remark 2 Obviously, one could extend the first Miquel mapping to the quadrangle consisting of I and the excenters E_i of Δ'' . If M traces a line l , then each of the excenters traces a curve l_{E_i} . Thereby, dependent on the line l and similar as in Fig. 5b, the centers E_i can change their roles. The combination of these four orbits l_{E_i} , l_1 seems to form a single algebraic curve.

2.3 Miquel circles and their midpoints

In the following we consider the triangle formed by the centers of the Miquel circles $m_A = k(AR'T')$, $m_B = k(BR'S')$, $m_C = k(CS'T')$. Independent of the chosen points R', S', T' we find a property of the centers of m_A, m_B, m_C (see Fig. 2, Fig. 7, and [16]), which we formulate as

Theorem 3 Given a triangle ΔABC and a triangle $\Delta R'S'T'$ arbitrarily inscribed to it. The centers M_A, M_B, M_C of the three Miquel circles m_A, m_B, m_C form a triangle similar to ΔABC . The similarity factor is $1/2 \cos \varepsilon$.

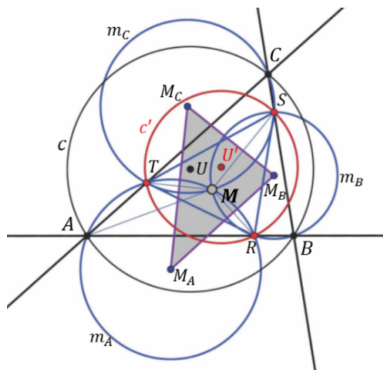


Figure 7: The triangle of the Miquel circle centers is similar to the given triangle ΔABC .

A proof of Theorem 3 can be read from Fig. 2. It follows that the sides of $\Delta M_A M_B M_C$ enclose a fixed angle with the sides ΔABC . We shall make use of Theorem 3 in the next chapters.

2.4 A second Miquel mapping

The circumcircle c' of triangle ΔRST intersects the sides of the initial triangle ΔABC in additional points $\bar{R}, \bar{S}, \bar{T}$ see Fig. 8. This new triangle $\Delta \bar{R}\bar{S}\bar{T} =: \bar{\Delta}$ gives rise to a new Miquel point \bar{M} , such that one can give:

Definition 3 Given a triangle ΔABC and arbitrarily chosen non collinear points R, S, T defining the Miquel point M . Let further $\bar{R}, \bar{S}, \bar{T}$ be the remaining intersections of the circumcircle c' of ΔRST with the sides of ΔABC , which define a new Miquel point \bar{M} , then we define the mapping $\mu_2 : M \mapsto \bar{M}$ as the second Miquel mapping.

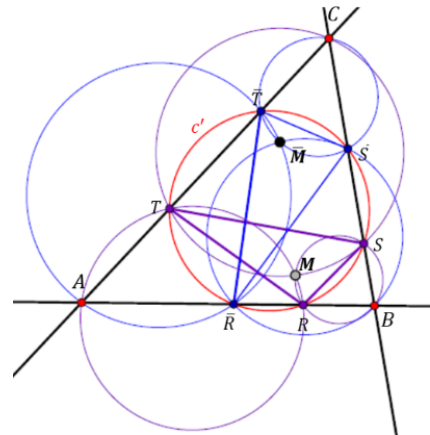


Figure 8: Visualization of the second Miquel mapping $\mu_2 : M \mapsto \bar{M}$.

If we consider the contact points $R = \bar{R}, S = \bar{S}, T = \bar{T}$ of in- and excircles of ΔABC then it becomes obvious that the incenter and the excenters of ΔABC are fixed points of the second Miquel mapping μ_2 .

We collect some properties of μ_2 , leaving the elementary but lengthy calculations to the reader.

A less obvious property, see Fig. 9, shall be formulated as

Theorem 4 Let the triangles $\Delta RST, \Delta \bar{R}\bar{S}\bar{T}$, both inscribed to ΔABC , have the same circumcircle c' . The touchinge midpoint triangles $\Delta_M := \Delta M_A M_B M_C$ and $\Delta_{\bar{M}} := \Delta \bar{M}_A \bar{M}_B \bar{M}_C$ of the therewith defined two triplets of Miquel circles are directly congruent with rotation center Z_2 and they are similar to the initial triangle ΔABC . Furthermore, the two Miquel points M, \bar{M} are equidistant to Z_2 and the angle $\angle MZ_2\bar{M}$ is twice the rotation angle $M_A \rightarrow \bar{M}_A$.

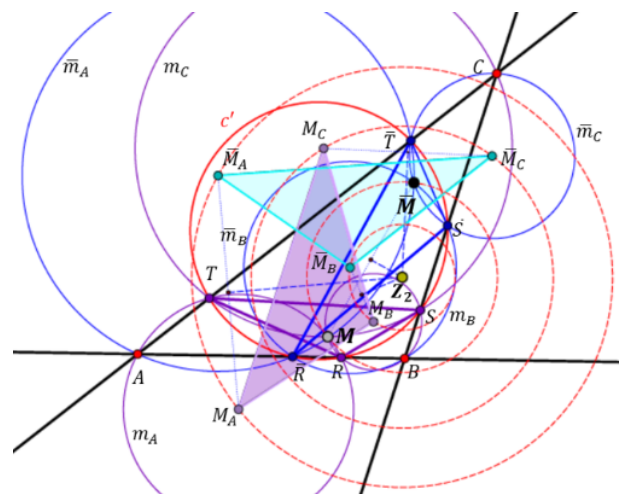


Figure 9: The midpoint triangles Δ_M and $\Delta_{\bar{M}}$ are directly congruent (rotation center Z_2) and similar to the initial triangle ΔABC .

When we start with a fixed (but arbitrarily chosen) Miquel point M and consider the one-parameter family of triangles, (in Fig. 10 represented by $\triangle RST$, $\triangle R'S'T'$), then we find the centers of their circumcircles on a line u , although these circles do form a pencil. They intersect the sides of $\triangle ABC$ in an additional family of triangles of type $\triangle \bar{R}\bar{S}\bar{T}$, $\triangle \bar{R}'\bar{S}'\bar{T}'$, which define a fixed Miquel point \bar{M} .

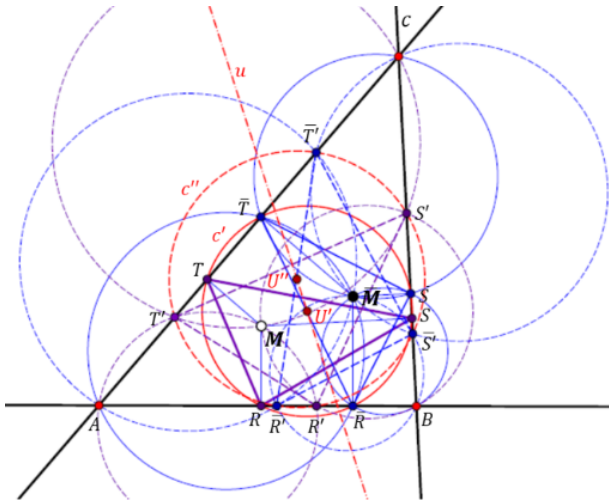


Figure 10: To a fixed Miquel point M belongs a set of triangles $\triangle RST$ and, via their circumcircles, a set of triangles $\triangle \bar{R}\bar{S}\bar{T}$, which again define a fixed Miquel point \bar{M} , such that $\mu_2 : M \mapsto \bar{M}$ is involutive.

Remark 3 For points M on the circumcircle $c = k(ABC)$ the points R, S, T are collinear and their circumcircle degenerates and splits to the line RS plus the ideal line ω , which defines the collinear triple $\bar{R}, \bar{S}, \bar{T}$. Therefore, as the circumcircles $k(\bar{A}\bar{R}\bar{T})$, $k(\bar{B}\bar{R}\bar{S})$, $k(\bar{C}\bar{S}\bar{T})$ are not defined, c is an exceptional set of points M .

We can therefore conclude

Theorem 5 The second Miquel mapping $\mu_2 : M \mapsto \bar{M}$ is involutoric. The in- and excenters of $\triangle ABC$ are fixed points of μ_2 , the circumcenter c of $\triangle ABC$ is an exceptional set of points M .

3 Special cases of Miquel’s theorem

3.1 The Theorems of Brocard

The French mathematician Henri Brocard (1845-1922) stated that the three circles passing through a pair of vertices of a triangle $\triangle ABC$ and touching one of its sides have a common point. Due to the two possible orientations of

\triangle there are two triples of circles, and therefore two such points, which are called *first* and *second Brocard point* B_1, B_2 , see e.g. [10]. They have many interesting properties and give rise to additional concepts, c.f. [7]. There is an interpretation in the sense of Miquel, if we choose R, S, T infinitely close to A, B, C . Then the Miquel circles will touch the sides of \triangle at its vertices and become *Brocard-Miquel circles* see Fig. 11. The two possible Miquel points become the first and second Brocard point B_1, B_2 . For these points, the Miquel stars pass through all three vertices of \triangle . Fig. 12 shows the situation for one of the Brocard points, but also for the altitude star.

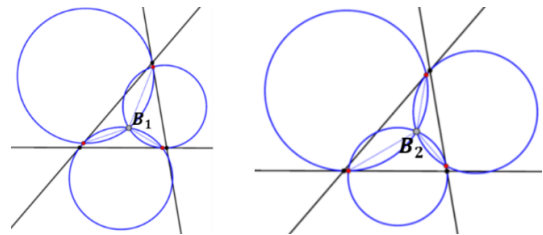


Figure 11: Brocard-Miquel circles and Brocard points of a triangle, as limit cases of Miquel points.

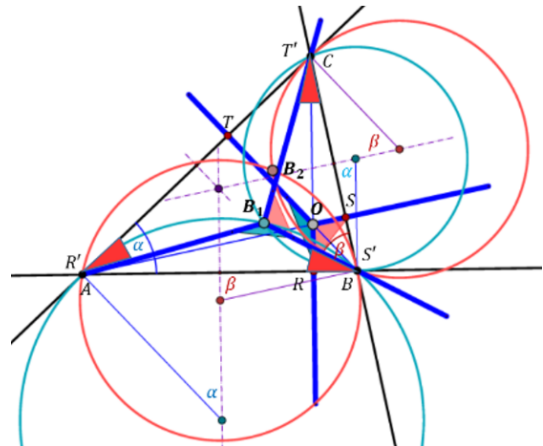


Figure 12: The Miquel-star through the three vertices of a triangle \triangle to Brocard point B_1 and to the orthocenter O .

As the sides of each Miquel star intersect the sides of a triangle at equal angles (see Fig. 2), the theorem concerning the so-called *fixed Brocard-angle* follows as a trivial corollary.

As for one limit triangle $\triangle RST$ its circumcircle c' coincides with the circumcircle c of \triangle , we get the triangle $\triangle \bar{R}\bar{S}\bar{T}$ mentioned in Chapter 2.2 as the 2nd limit triangle, such that the Miquel points B_1 and B_2 correspond in the second Miquel mapping μ_2 . We formulate this as

Theorem 6 The Brocard points B_1 and B_2 of a triangle $\triangle ABC$ correspond in the involutive Miquel mapping μ_2 of $\triangle ABC$.

We consider now the midpoints of the two triads of Brocard-Miquel circles b_i^A, b_i^B, b_i^C , ($i = 1, 2$), which intersect in the Brocard points B_i . As a consequence of Theorem 4 and by arguments of congruent angles, see Fig. 13 and 14, we can formulate

Theorem 7 *The centers Z_i^X , ($i = 1, 2; X = A, B, C$), of the two triplets of Brocard Miquel circles b_i^X form two congruent triangles Δ_1, Δ_2 , which are similar to the given triangle ΔABC . They are in Desargues-position with the circumcenter U of Δ as perspector and the bisector of the segment $[B_1, B_2]$ as perspectrix (passing through U). The centers Z_i^X of the 6 Brocard-Miquel circles b_i^X lay in pairs on circles, which are concentric with the circumcircle z of the isosceles triangle ΔB_1UB_2 .*

The proof of Theorem 7 can be performed by straight forward calculation similar to that of the first and second Miquel mappings. The similarity statement is a consequence of Theorem 3.

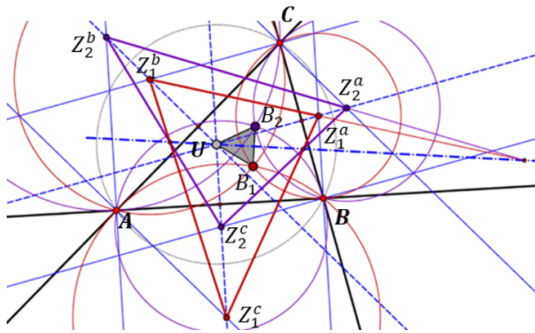


Figure 13: The midpoints of the two triplets of Brocard-Miquel circles form two congruent triangles of a Desargues configuration. They are similar to the initial triangle.

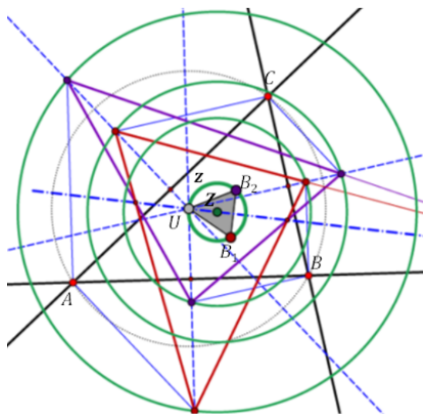


Figure 14: The midpoints of the two triads of Brocard-Miquel circles are in pairs on concentric circles. Their common center is the center Z of the circumcircle z of ΔB_1UB_2 .

Remark 4 *It turns out that the similarity factor σ for the midpoint triangles $\Delta'_i = \Delta Z_i^A Z_i^B Z_i^C$ with respect to Δ becomes $\sigma = \overline{UB_1} : \overline{B_1B_2}$. Consequently, one could construct the Brocard points for these triangles, and we must receive Brocard triangles similar to ΔB_1UB_2 . Fig. 15 shows the situation for the midpoint triangle Δ'_i , which is directly similar to Δ . Taking $\Delta ABC = \Delta A^0 B^0 C^0$ and $\Delta B_1UB_2 = \Delta B^0_1 U^0 B^0_2$ as the initial situation, the next step delivers $B^1_1 = U^0, B^1_2 = B^0_2$, and we get a chain of similar triangles with common vertex $B^0_2 = \dots = B^n_2$. Constructing the Brocard points for both midpoint triangles at each stage gives a kind of a fractal structure based on a bifurcation process.*

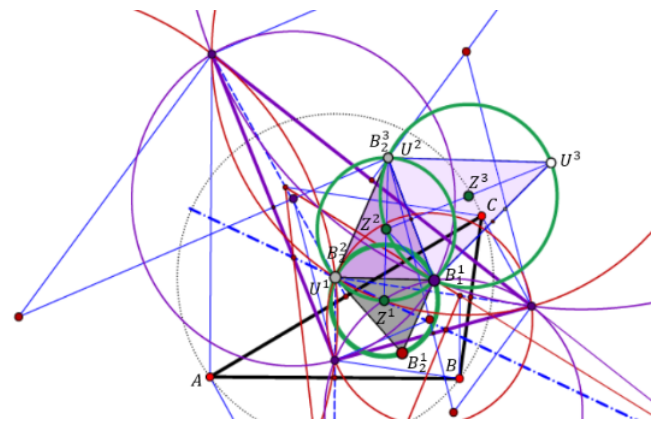


Figure 15: The midpoint triangles Δ_1, Δ_2 are similar to the given triangle. The similarity factor σ turns out to be the ratio $\overline{UB_1} : \overline{B_1B_2}$.

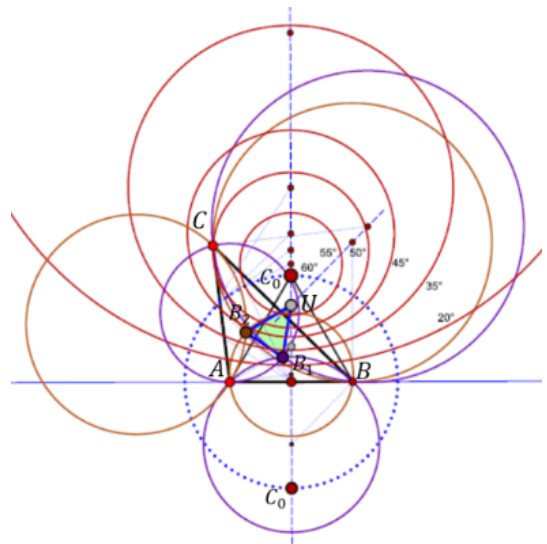


Figure 16: Vertices C moving along circles of a hyperbolic pencil of circles, together with fixed vertices A, B , form triangles with similar triangles ΔB_1UB_2 .

Remark 5 As a triangle \triangle needs three parameters to be described, while $\triangle B_1UB_2$ is isosceles, there must be a one-parameter family of triangles to a given triangle $\triangle B_1UB_2$. We formulate the result when keeping the vertices A and B fixed and C movable such that the corresponding triangles $\triangle B_1UB_2$ are similar, see Fig. 16:

Theorem 8 The vertices C to fixed vertices A, B move along two circles symmetric to the line AB if we demand that the corresponding triangles $\triangle B_1UB_2$ shall be similar. The circles $c(\varphi)$ to different angles $\varphi = \sphericalangle B_1UB_2$ belong to a hyperbolic pencil of circles, the degenerate circles of which are the two possible vertices C forming equilateral triangles $\triangle ABC$ over the segment $[AB]$.

We omit the proof, which is straight forward calculation similar to that for μ_1 and μ_2 . A consequence of Theorem 8 is that $0^\circ < \varphi < 60^\circ$. Therefore, only for equilateral triangles \triangle the triangles \triangle_1, \triangle_2 coincide and are congruent to \triangle .

3.2 The points R, S, T fulfill the Menelaos condition

As a second special case we choose collinear points R, S, T . In other words, R, S, T fulfill Menelaos’s condition. Now $\triangle RST =: \triangle'$ is degenerate and the, in general, three parabolas (Fig. 3) coincide in a single one with the Miquel point M as focus, see Fig. 17.

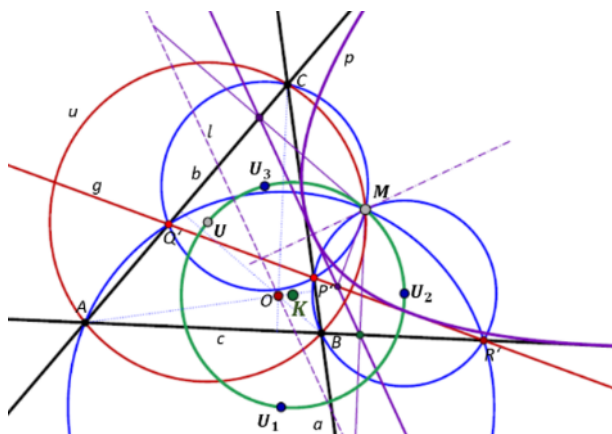


Figure 17: Collinearly chosen points R, S, T lead to the theorems of Steiner and Simson-Wallace and of Kantor.

J. Steiner interpreted the line RS as the fourth line of a quadrilateral and stated that the four circumcircles of its four partial triangles intersect in one point, namely the focus of the single parabola p touching all four lines. In the sense of Miquel, all possible Miquel triangles $\triangle R'S'T'$ to M must be degenerate and M is a point of the circumcircle of \triangle . The pedal points of M at the sides of $\triangle ABC$ are

therefore collinear with the vertex tangent of the parabola p , which means that the theorem of Simson-Wallace (see [4]) becomes an obvious consequence. As the Miquel points are restricted to the circumcenter of \triangle , i.e. a one-parameter set, while for the line RS there is a two parameter set of possibilities, there must be a one-parameter set of lines belonging to the same Miquel point M . Indeed, this set consists of the tangents of the single parabola mentioned above. Of course, one again could define a kind of Miquel mapping $\mu^* : g \rightarrow M$, which now is singular with image $\text{img}(\mu^*) = u$ and the tangent sets of parabolas as fibers.

Remark 6 It seems worth mentioning a theorem by S. Kantor [9], which states that the centers U, U_1, U_2, U_3 of the four circumcircles of the partial triangles of a quadrilateral and their common intersection, (the Miquel point M) are concyclic. In Fig. 17 the center of this Kantor circle is labelled by K . Kantor considered the five partial quadrilaterals of a five-lateral and states that the centers of the five Kantor circles are again concyclic, delivering a new center. K. Hirano [6] considers these new centers of a six-lateral and found that they again are concyclic. Finally, Ch. J. Hsu [17] extended these results step by step to n -laterals, stating that concyclicity prevails in each step. Furthermore, a connection of Steiner’s and Miquel’s theorems is applied in [11] to define so-called Steiner-Miquel mappings.

3.3 The points R, S, T fulfill Ceva’s condition

Now, we choose R, S, T such that $RC, SA,$ and TB meet at a point X , which means that they fulfill the “Ceva condition”. Even though this case looks somehow dual to the former case and can be related to it via the triangle polarity to $\triangle ABC$, it has quite different properties.

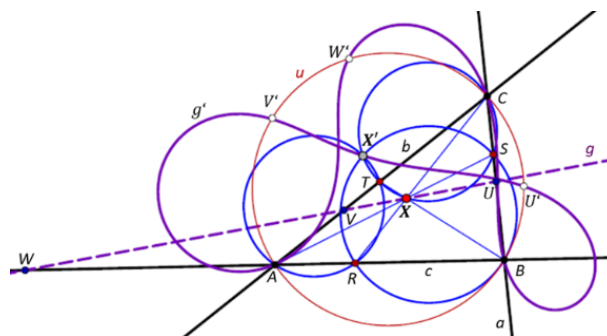


Figure 18a: The 2^nd Miquel-mapping $\mu_2 : X \mapsto X'$ maps a line g to a curve g' of degree 6. If g coincides with a side of \triangle , then its μ_2 -locus is the circumcircle u of $\triangle ABC$.

Now, a mapping of some point X to the Miquel point $M =: X'$ is induced in a natural way which is algebraic of degree 6. In the following, we give a description of what shall be called *third Miquel-mapping* $\mu_3 : X \mapsto X'$. It turns

out that points on the sides of $\triangle ABC$ are mapped to points of the circumcircle of this triangle \triangle , see Fig. 18a.

In the view of circle geometry, which usually considers both lines and circles as Möbius circles within a projective line over complex numbers, and which is modeled as the Gauss plane π and/or the Riemannian sphere, we present here a slight modification of this approach: We replace the Riemannian sphere by a paraboloid of revolution and an axis normal to the plane of the triangle \triangle . The standard *stereographic projection* of the Riemann sphere becomes then the orthogonal projection onto what shall be called *Riemann paraboloid* Ψ described by the Cartesian equation

$$\Psi : x^2 + y^2 = z. \tag{5}$$

For a convenient calculation, we embed the Euclidean space into its projective closure and use homogeneous coordinates $(x, y, z) \mapsto (x_0, x_1, x_2, x_3) \mathbb{R}$. Let the Euclidean planar coordinate representation of the vertices of triangle \triangle and of the points R, S, T be $A := (0, 0)$, $B := (1, 0)$, $C := (u, v)$, $R := (r, 0)$, $S := (1 + (u - 1)s, vs)$, $T := (ut, vt)$.

They are mapped by the *inverse stereographic projection* $p : \pi \rightarrow \Psi$ to points $A^p, \dots, T^p \in \Psi$. The representation in homogeneous coordinates of these image points reads therefore as

$$\begin{aligned} A^p &= (1, 0, 0, 0) \mathbb{R} \\ B^p &= (1, 1, 0, 1) \mathbb{R}, \\ C^p &= (1, u, v, u^2 + v^2) \mathbb{R} \\ R^p &= (1, r, 0, r^2) \mathbb{R} \\ T^p &= (1, ut, vt, (u^2 + v^2)t^2) \mathbb{R} \\ S^p &= (1, 1 + u_{-1}s, vs, (1 + u_{-1}s)^2 + v^2s^2) \mathbb{R}, \quad (u_{-1} := u - 1). \end{aligned} \tag{6}$$

The planes $A^pR^pT^p$, $B^pS^pR^p$, $C^pT^pS^p$ represent the three Miquel circles, and, because of Miquel's theorem, their intersection point M^p must be a point of Ψ .

As there is a one-parameter family of triplets R, S, T to a given Miquel point X' , we can expect, that at least one of those triplets fulfills Ceva's condition, such that it is possible to define the inverse mapping $\mu_2^{-1} : X' \rightarrow X$ in a geometric way, see Fig. 18b. Starting with an arbitrarily given triple R', S', T' , we construct a *Ceva trilateral* with sides AS' , BT' , CR' and its vertices U', V', W' . When rotating the Miquel star (Fig. 2), these vertices trace conics with a common point X , the Ceva point of X' .

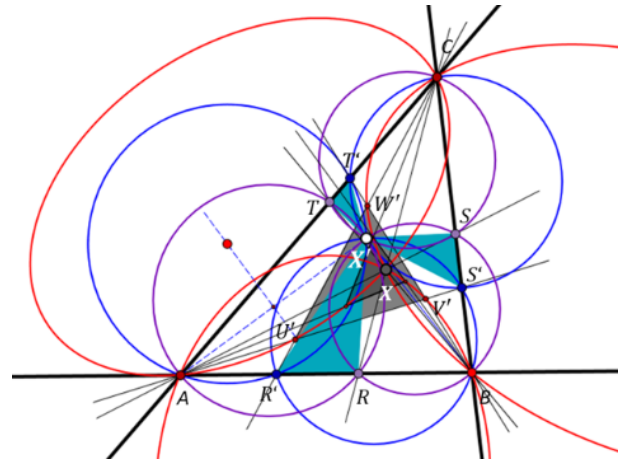


Figure 18b: Reconstruction of the Ceva point X to a given Miquel point X' .

Theorem 9 *The Ceva-Miquel mapping $\mu_3 : X \mapsto X'$ maps a Ceva point to a Miquel point. It is invertible and has the orthocenter of $\triangle ABC$ as fixed point.*

4 Orbits of Miquel points for special sets of Miquel triangles $\triangle RST$

In the earlier Chapter 3.3, Fig. 15, we considered a special kind of dependencies of the point triples (R, S, T) caused by the fact that the corresponding Ceva points X are bound to a line g . In this chapter, we shall look for other and simpler kind of dependencies. As there are too many quite interesting cases, they shall be treated in a separate paper. Here, we restrict ourselves to present the case of R, S, T running through similar point series on the sides of $\triangle ABC$, see Fig. 19. This shall mean that the ratios, in cyclic order, are equal, i.e. $\text{ar}(ARB) = \text{ar}(BSC) = \text{ar}(CTA) =: t \in \mathbb{R}$. We formulate

Theorem 10 *The Miquel points M to triplets (R, S, T) at sides of a triangle $\triangle ABC$ fulfilling the ratio equality $\text{ar}(ARB) = \text{ar}(BSC) = \text{ar}(CTA) =: t \in \mathbb{R}$ trace the 1st Brocard circle, which is the circumcircle of the triangle formed by the circumcenter U and the two Brocard points B_1, B_2 of \triangle .*

It turns out that this Brocard circle contains the triangle centers X_i with the following Kimberling numbers i (see [10]):

- $i \in \{3, 6, 1083, 1316, 1670, 1671, 2555, 2556, 2557, 32481, 32482, 5091, 5108, 6232, 6322, 6795, 8429, 9129, 11650, 13414, 13415, 13511, 13515, 13516, 14685, 18332, 18338, 24279, 35901, 43765, 46407, 46410, 53719, 59781, 59782, 59783, 59784, 59785, 59786, 59787, 59788, 59789, 59790, 59791, 59792, 59793, 59794, 59795, 59796\}$.

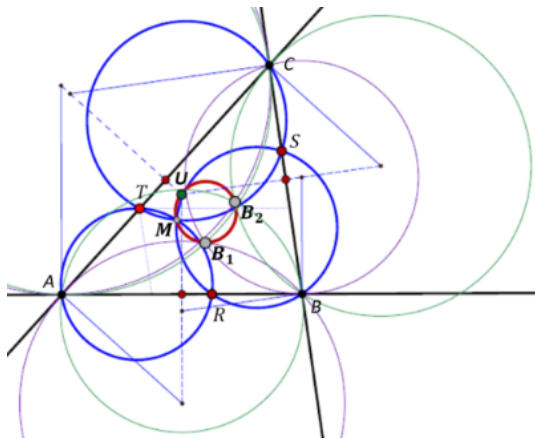


Figure 19: The set of triplets R, S, T with $ar(ARB) = ar(BSC) = ar(CTA) =: t \in \mathbb{R}$ has its Miquel points on the Brocard circle of $\triangle ABC$.

In addition we found (see Fig. 20)

Theorem 11 The cases of dependencies of R, S, T , with $ar(ARB) = t \in \mathbb{R}$, and $ar(BSC) = f_S(t)$, $ar(CTA) = f_T(t)$, where the linear functions $f_S(t)$, $f_T(t)$ lead to circles as loci of Miquel points.

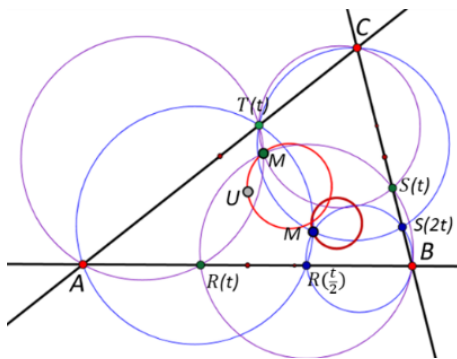


Figure 20: The set of triples R, S, T with $ar(ARB) = t$, $ar(BSC) = f_S(t)$, $ar(CTA) = f_T(t)$, where $f_S(t)$, $f_T(t)$ are linear functions, causes the Miquel points to lie on a circle.

5 Miquel’s theorem in circle geometries and Minkowski planes

5.1

It is near to consider the classical version of the Theorem of Miquel in the Möbius-Gauss plane and use it as an axiom for certain ring geometries, see [2]. There is an interpretation as a $(6_4, 8_3)$ -configuration of 6 Möbius circles, each containing four points, and eight Möbius points, each on three Möbius circles. Via stereographic projection onto

the Riemann sphere, these eight points can be seen as the vertices of a right prism, e.g., a cube, while its six faces act as the planes of the circumcircles of face rectangles, see Fig. 21a.

Similarly, the four (congruent) circles of the so-called beermat theorem (Fig. 21b, left), in some sense also a relative to Miquel’s configuration, form a $(4_3, 4_3)$ -configuration and can be interpreted as an image of a tetrahedron, see Fig. 21b. The beermat theorem states that, if one marks three points A, B, C on a circle c and draws congruent circles c_1, c_2, c_3 through any pair of these points, then these three circles have a common point which turns out to be the orthocenter of $\triangle ABC$.

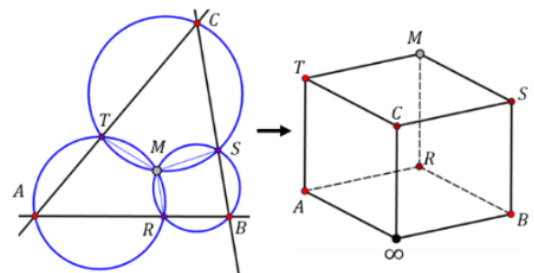


Figure 21a: The $(6_4, 8_3)$ -configuration of a Miquel figure is interpreted as vertices and faces of a cube.

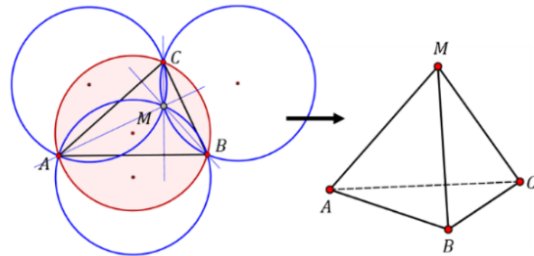


Figure 21b: The $(4_3, 4_3)$ -configuration of a beermat figure can be interpreted as vertices and faces of a tetrahedron.

Remark 7 If we choose R, S, T as the feet of the altitudes of $\triangle ABC$, then the orthocenter O becomes the corresponding Miquel point. We can say that this combines somehow the beermat configuration with Miquel’s configuration. In addition to the altitudes r, s, t , which now contain 4 points, also the Thales circles over $[AB]$, $[BC]$ and $[CA]$ pass through 4 points, see Fig. 22. This gives rise to a $(12_4, 8_6)$ -configuration which allows an interpretation as the 8 vertices of a cube, its 6 faces and 6 diagonal planes. In Fig. 22 the altitudes r, s, t are mapped to diagonal planes ρ, σ, τ through the vertex labelled as ∞ . This shows that the standard interpretation of Miquel’s configuration by a cube can only be a metaphor, as the cube automatically

has additional planes through four vertices, and this would mean six additional Möbius circles containing four points also in the general Miquel figure.

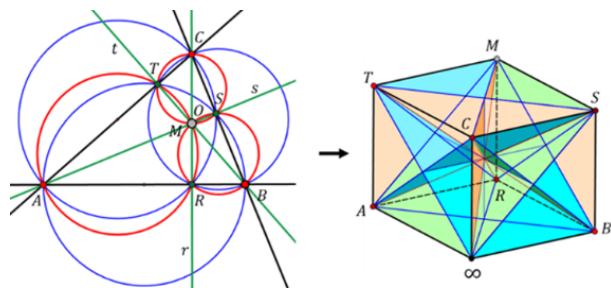


Figure 22: The $(12_4, 8_6)$ -configuration of the special Miquel figure with the orthocenter as Miquel point can be interpreted as vertices and faces and diagonal planes of a cube.

Steiner’s configuration with its 4 straight Möbius circles and 4 Miquel-Möbius circles is therefore an $(8_4, 8_4)$ -configuration. Here, no proper interpretation of a polyhedron in 3-space with quadrangular faces / diagonal planes is possible. One could still use a cube and 8 tetrahedra, the four vertices of which symbolizing concyclic point quadruples, see Fig. 23a.

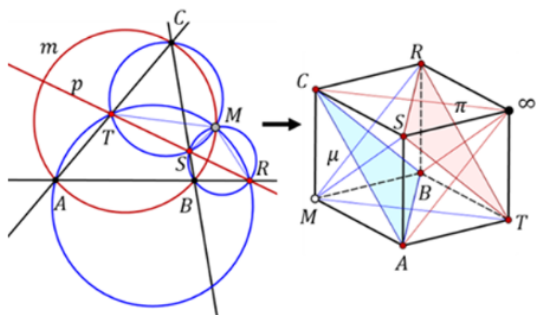


Figure 23a: The $(8_4, 8_4)$ -configuration of the Steiner figure could be interpreted as the 8 vertices of a cube with 8 partial tetrahedra, the vertices of which correspond to concyclic point quadruples.

Each of the two Brocard figures Fig. 11 show a degenerate situation, where three points, the vertices of $\triangle ABC$, count twice (and lead to parabolic pencils of circles), while two points are always distinct. In this case we can no longer speak of a configuration. We get six Möbius circles and five points, and a 3D-interpretation could be the six planes and five points of a three-sided double pyramid, see Fig. 23b.

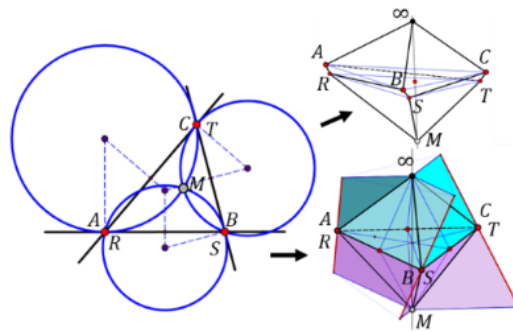


Figure 23b: “Limit situation“ for one of the Brocard figures. It is no longer a con-figuration, it can be interpreted as a 3-sided double-pyramid.

5.2

Affine planes with a norm are called *Minkowski planes*. Here, a centrally symmetric and convex curve or polygon acts as *unit circle* u with radius of length 1 and all circles are centric similar or translates to u , see e.g. [1] and [15]. Therewith, the question arises, if there are analogs to the classical figure of Miquel and its relatives, see e.g. [1] and [14]. Note that the norm depends on an additionally given (affine) coordinate frame, see Fig. 24, while the (geometric) distance measure is already well-defined by u alone.

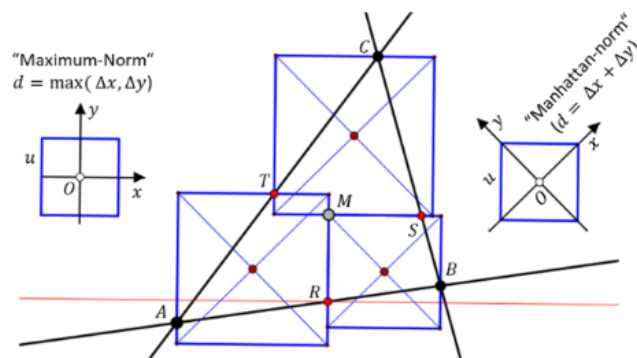


Figure 24: Miquel figure for a parallelogram as unit circle u . Dependent on the affine coordinate frame, it allows an interpretation in a plane with maximum norm or with Manhattan norm.

For the beermat theorem to remain valid, central symmetry of u is a sufficient condition. For some triples R, S, T , one of the three beer mats through R, S or S, T or T, R is identical with the basic beer mat u . Fig. 25a and 25b show this for beer mats being regular hexagons, decagons, and pentagons.

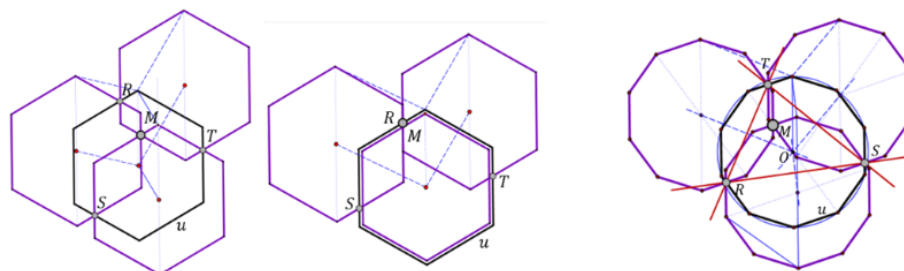


Figure 25a: The beermat theorem is valid in Minkowski planes.

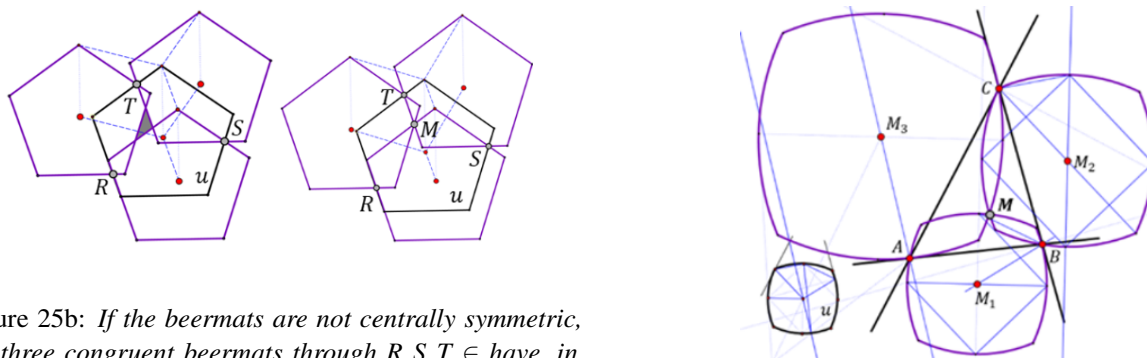


Figure 25b: If the beermats are not centrally symmetric, the three congruent beermats through $R, S, T \in$ have, in general, no common point, but there exist triplets R, S, T such that they can have a common point M .

It turns out that there is, in general, no analogon for the Steiner-Wallace-Simson figure in Minkowski planes with a unit circle u different from an ellipse. The same is true also for Brocard's theorem. To translate a Brocard figure into a Minkowski plane the unit circle u should be strictly convex and smooth, such that e.g. the left-orthogonality of Birkhoff [3] becomes a (1,1)-relation. In general, the three Brocard-Miquel circles to a given triangle $\triangle ABC$ have no common point, see Fig. 26a, but there are triangles $\triangle ABC$ and unit circles u , such that they can be concurrent, see Fig. 26b.

Figure 26b: A special case of a Brocard figure, where the three Brocard-Miquel circles pass through one point M .

5.3

Finally, we shortly point to some classical Cayley-Klein planes, thus generalizing the Euclidean case in an obvious direction. As long as we deal with pseudo-Euclidean and isotropic planes the place of action is a projectively extended affine plane and we can expect that Miquel's theorem and its relatives remain valid. For example, the isotropic case of a Miquel figure is shown in Fig. 27a, while Fig. 27b shows an isotropic version of the Steiner-Wallace-Simson figure.

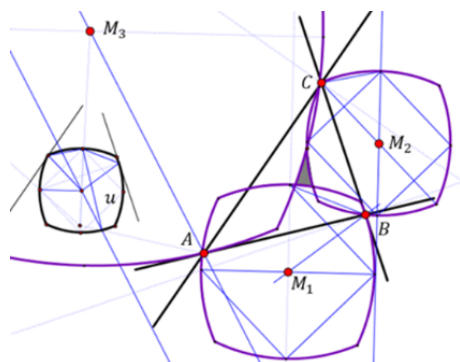


Figure 26a: A general case for a Brocard figure in a Minkowski plane with unit circle u . The three Brocard-Miquel circles have no common point.

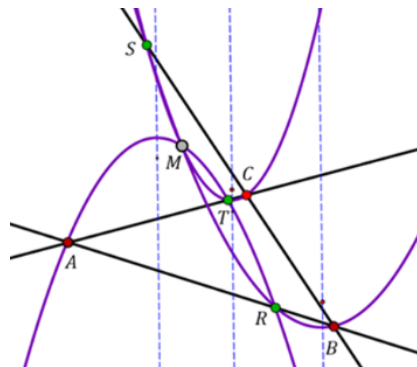


Figure 27a: A Miquel figure in an isotropic plane.

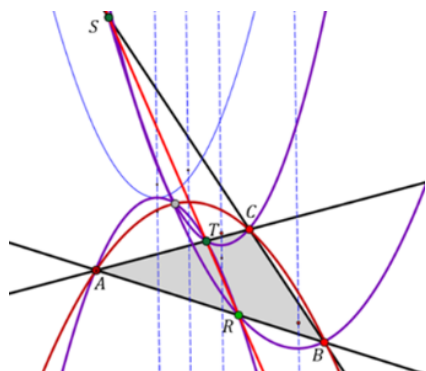


Figure 27b: A “Steiner figure” with collinear points R, S, T .

In an elliptic or hyperbolic plane a triangle has four circumcircles. A Miquel figure in such a plane consists of the triangle $\triangle ABC$, the triplet R, S, T on its sides, and the four times three circumcircles of partial triangles. It is well-known that there are, in general, no common points for triplets of such circles, such that Miquel's Theorem is not true in such planes.

Also the beermat theorem, dealing with congruent circles, is not true in elliptic or hyperbolic planes, as can be seen in Fig. 28: The three congruent circles through R, S resp. S, T resp. T, R , ($R \neq S \neq T$ arbitrarily chosen points of a fixed circle c), have no common point, and they do not pass through the orthocentre of $\triangle RST$.

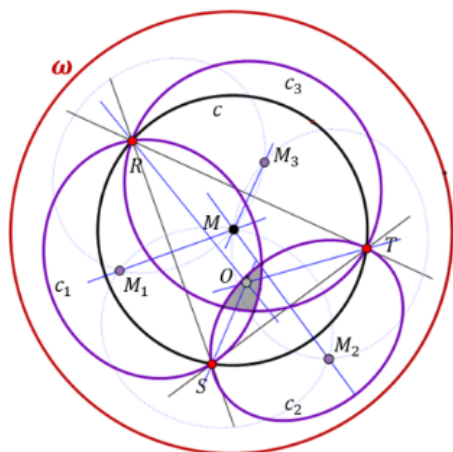


Figure 28: Four hyperbolic congruent circles c_i forming a beermat figure visualized in the Klein model of a hyperbolic plane with absolute conic ω .

6 Final remarks

Some of the material treated here is more or less common knowledge. However, we shall emphasize the connections

between several elementary geometric theorems, and their interpretation as special cases of Miquel's Theorem. This leads, on one hand, to some Miquel mappings, which are seemingly new, and on the other to a more detailed understanding of those standard theorems.

The figures in this paper are generated with the graphics freeware *Cinderella* [5], an effective tool for planar geometry in Euclidean, hyperbolic and elliptic geometry.

Acknowledgments

The authors thank the reviewers for valuable comments and proposed improvements.

References

- [1] ASPLUND, E., GRÜNBAUM, B., On the Geometry of Minkowski planes, *Enseign. Math.* **6** (1960), 299–306.
- [2] BENZ, W., *Vorlesungen über Geometrie der Algebren*, Springer, Berlin, 1973, <https://doi.org/10.1007/978-3-642-88670-6>
- [3] BIRKHOFF, G., Orthogonality in linear metric spaces, *Duke Math. J.* **1**(2) (1935), 169–172, <https://doi.org/10.1215/S0012-7094-35-00115-6>
- [4] BLAŽEK, J., PECH, P., Generalization of Simson–Wallace theorem: planar and spatial formulation, *J. Geom.* **114**, 5 (2023), <https://doi.org/10.1007/s00022-022-00665-z>
- [5] CINDERELLA, *Die interaktive Geometrie-Software Cinderella, Multiscale Modeling & Simulation*, <https://cinderella.de/tiki-index.php> (last access August 2024)
- [6] HIRANO, K., On some center circles and their relations, *Sugaku* **8** (1956/57), 210–211.
- [7] HONSEGER, R., The Brocard angle, *Episodes in Nineteenth and Twentieth Century Euclidean geometry*, Math. Assoc. of America 1995, 101–106, <https://doi.org/10.5948/UP09780883859513>
- [8] HSU, CH. J., On systems of center-circles derived successively from that of Steiner-Kantor-Morley, *Soochow J. Math. Natur. Sci.* **3** (1977), 17–34.
- [9] KANTOR, S., Über das vollständige Fünfseit, *Sb. Österr. Akad. Wiss.* **78** (1878), 1–9.
- [10] KIMBERLING, C., *Encyclopedia of Triangle Centers*, <https://faculty.evansville.edu/ck6/encyclopedia/etc.html> (last access June 2024)

- [11] MACKAY, J.S., The Wallace line and the Wallace point, *Proc. Edinb. Math. Soc.* **9** (1890), 83–91, <https://doi.org/10.1017/S001309150003087X>
- [12] MIQUEL, A., Théorèmes sur les intersections des cercles et des spheres, *J. Math. Pures Appl.* **3** (1838), 517–522.
- [13] ODEHNAL, B., A Miquel-Steiner Transformation, *KoG* **27** (2023), 14–24, <https://doi.org/10.31896/k.27.2>
- [14] SPIROVA, M., On Miquel's theorem and inversions in normed planes, *Monatsh. Math.* **161** (2010), 335–345, <https://doi.org/10.1007/s00605-009-0153-8>
- [15] THOMPSON, A.C., *Minkowski Geometry*, Cambridge University Press, 1996, <https://doi.org/10.1017/CB09781107325845>
- [16] DE VILLIERS, M., A variation of Miquel's theorem and its generalization, *Math. Gaz.* **98**(542) (2014), 334–339, <https://doi.org/10.1017/S002555720000142X>
- [17] WEISS, G., 3D-Versions of Theorems related to Miquel's Theorem, *Proceedings of the Slovak-Czech Conference on Geometry and Graphics 2023* (Kremnica, Slovakia, Sept. 11-14, 2023), Bratislava 2023, 195–202.

Gunter Weiss

orcid.org/0000-0001-9455-9830

e-mail: weissgunter@gmx.at

University of Technology Vienna
Karlsplatz 13, 1040 Vienna, AustriaUniversity of Technology Dresden
Helmholtzstraße 10, 01069 Dresden, Germany**Boris Odehnal**

orcid.org/0000-0002-7265-5132

e-mail: boris.odehnal@uni-ak.ac.at

University of Applied Arts Vienna
Oskar-Kokoschka-Platz 2, 1010 Vienna, Austria